

An oncogene regulating chromatin favors response to immunotherapy

Oncogene CHAF1A and immunotherapy outcomes

Leqian Ying^{a,b}, Zhangmin Hu^a, Yi Lu^c, Qing Tao^a, Fen Xiong^a, Yongqian Shu^d, Yufei Yang^a, Xuehan Qiao^a, Chen Peng^a, Yuchun Jiang^a, Miao Han^a, Min Xu^e, Xiaoqin Li^a, and Deqiang Wang^{id}^a

^aDepartment of Oncology, Digestive Disease Institute&Cancer Institute of Jiangsu University, Affiliated Hospital of Jiangsu University, Zhenjiang, China; ^bDepartment of Oncology, Zhong-Da Hospital, Medicine School, Southeast University, Nanjing, China; ^cDepartment of Oncology, Wujin Hospital Affiliated with Jiangsu University, Changzhou, China; ^dDepartment of Oncology, Jiangsu Province Hospital & The First Affiliated Hospital of Nanjing Medical University, Nanjing, China; ^eDepartment of Gastroenterology, Digestive Disease Institute of Jiangsu University, Affiliated Hospital of Jiangsu University, Zhenjiang, China

ABSTRACT

Many biological processes related to cell function and fate begin with chromatin alterations, and many factors associated with the efficacy of immune checkpoint inhibitors (ICIs) are actually downstream events of chromatin alterations, such as genome changes, neoantigen production, and immune checkpoint expression. However, the influence of genes as chromatin regulators on the efficacy of ICIs remains elusive, especially in gastric cancer (GC). In this study, thirty out of 1593 genes regulating chromatin associated with a favorable prognosis were selected for GC. CHAF1A, a well-defined oncogene, was identified as the highest linkage hub gene. High CHAF1A expression were associated with microsatellite instability (MSI), high tumor mutation burden (TMB), high tumor neoantigen burden (TNB), high expressions of PD-L1 and immune effector genes, and live infiltration of immune cells. High CHAF1A expression indicated a favorable response and prognosis in immunotherapy of several cohorts, which was independent of MSI, TMB, TNB, PD-L1 expression, immune phenotype and transcriptome scoring, and improved patient selection based on these classic biomarkers. *In vivo*, CHAF1A knockdown alone inhibited tumor growth but it impaired the effect of an anti-PD-1 antibody by increasing the relative tumor proliferation rate and decreasing the survival benefit, potentially through the activation of TGF- β signaling. In conclusion, CHAF1A may be a novel biomarker for improving patient selection in immunotherapy.

ARTICLE HISTORY

Received 10 September 2023
Revised 31 December 2023
Accepted 2 January 2024

KEYWORDS

Cancer; CHAF1A; immune checkpoint; immunotherapy; oncogene



Background

In recent years, immunotherapy, represented by immune checkpoint inhibitors (ICIs), has been a major breakthrough in the field of tumor therapy. One of its main mechanisms is to relieve immunosuppression induced by the binding of programmed cell death receptor-1 (PD-1) to its ligand, PD-L1.¹ Recently, ICIs have been tested in the first-line treatment of metastatic gastric cancer (GC), including in four pivotal phase III trials (KEYNOTE-062, CheckMate 649, ATTRACTION-4, and ORIENT-16). Specifically, the CheckMate 649 global phase III trial showed that the combination of nivolumab and chemotherapy significantly prolonged progression-free survival (PFS) and overall survival (OS) compared to chemotherapy alone in patients with PD-L1 combined positive score (CPS) ≥ 5 and in the entire population.² However, a graphical algorithm to reconstruct unreported Kaplan-Meier (KM) plots of PD-L1 CPS subgroups in CheckMate 649 found that patients with CPS 1–4 did not benefit from first-line nivolumab plus chemotherapy.³


It seems that the PD-L1 CPS score was a useful predictive biomarker for determining immunotherapy efficacy in GC. However, there are some limitations to its application in the

real world. First, the CPS cutoff value is controversial, which is used as five in treatment with nivolumab but as 10 in single pembrolizumab therapy.^{2,4,5} Second, the antibodies used to evaluate PD-L1 expression are different between nivolumab and pembrolizumab, whose interchangeability needs validations.⁶ Third, intra-tumor heterogeneity means that biopsy assessment may not accurately represent the overall tumor status.⁷ Moreover, PD-L1 expression in cells undergoes dynamic changes, indicating that its assay result also changes over time.⁸ Other commonly used biomarkers for the therapeutic efficacy of ICIs mainly include microsatellite instability (MSI) and tumor mutation burden (TMB). MSI is a strong and well-established predictor, but its occurrence is rare, even in gastrointestinal tumors.⁹ TMB level lacks unified standards, and its relationship with immunotherapy efficacy is still controversial.¹⁰ Therefore, it is still necessary to identify novel biomarkers to improve patient selection for immunotherapy in GC and other tumors.

The traditional view of therapy resistance in cancer is centered around the derepression or loss of certain genes, either caused by driver mutations or by epigenetic disruptions.

CONTACT Deqiang Wang  deqiang_wang@aliyun.com  Department of Oncology, Digestive Disease Institute&Cancer Institute of Jiangsu University, Affiliated Hospital of Jiangsu University, Zhenjiang 212001, China

LY, ZH, and YL are joint first authors.

 Supplemental data for this article can be accessed online at <https://doi.org/10.1080/2162402X.2024.2303195>

© 2024 The Author(s). Published with license by Taylor & Francis Group, LLC.

This is an Open Access article distributed under the terms of the Creative Commons Attribution-NonCommercial License (<http://creativecommons.org/licenses/by-nc/4.0/>), which permits unrestricted non-commercial use, distribution, and reproduction in any medium, provided the original work is properly cited. The terms on which this article has been published allow the posting of the Accepted Manuscript in a repository by the author(s) or with their consent.

Chromatin abnormalities, on the other hand, have a more significant and undetectable influence on genetic expression.¹¹ In eukaryotes, genetic information is stored in chromatin, an ensemble of DNA, histones, and several non-histone proteins. Cellular DNA is entirely accommodated in the nucleus through necessary compaction based on hierarchical chromatin organization. The chromatin structure is continuously modified to maintain informational continuity by regulating access to transcriptional, repair, or replicative factors. Therefore, chromatin organization and remodeling play regulatory roles in many processes related to cancer development, including DNA replication stress, DNA damage response, cell cycle, cell senescence, cell death, metastasis, angiogenesis, and anti-tumor immunity.^{11–14} Recently, targeting factors to disrupt chromatin organization and remodeling has become a promising strategy to combat cancer.^{12,13} Moreover, studies have shown that genetic alterations in the SWItch/sucrose nonfermentable (SWI/SNF) chromatin remodeling complex foster resistance to ICIs.^{14,15}

It is still unclear whether genes playing a role in chromatin regulation affect the outcomes of GC patients treated with ICIs. In this study, we screened these genes to identify potential biomarkers for predicting the effectiveness of ICI in GC. We found that chromatin assembly factor 1 (CAF-1) subunit A (CHAF1A), was significantly associated with immune characteristics and infiltration of immune cells in GC and other tumors. High CHAF1A expression indicates favorable outcomes of ICI treatment. Interestingly, as a known oncogene,¹⁶ CHAF1A knockdown impaired the effect of an anti-PD-1 antibody *in vivo*, possibly through the activation of TGF- β signaling.

Patients and methods

Patients

Four GC cohorts were used to screen for chromatin-associated genes, including the Asian Cancer Research Group (ACRG), The Cancer Genome Atlas (TCGA), GSE15459, and GSE57303 cohorts. A GC cohort from The Affiliated Hospital of Jiangsu University (AHJU) was used to validate the role of specific genes.^{17–20} Three immunotherapy cohorts were used: the NCT#02589496 cohort, wherein the GC participants had received second-line PD-1 inhibition with pembrolizumab²¹; the AHJU immunotherapy cohort, wherein GC participants were treated with the first-line combination of chemotherapy with anti-PD-1 antibodies such as sintilimab, tislelizumab, or camrelizumab; and the IMvigor210 cohort, wherein patients with metastatic urothelial cancer (mUC) were treated with the anti-PD-L1 antibody atezolizumab.²² Therapy response was evaluated according to Response Evaluation Criteria in Solid Tumors (RECIST) 1.1. The enrollment criteria for patients included: 1) pathological diagnosis of GC; 2) available expression data or available samples for genetic testing; and 3) no prior history of anticancer therapies before genetic testing. Clinical and pathological staging and classification were adopted from the American Joint Committee on Cancer criteria. The ethics committee of the AHJU approved the research protocol, and all patients from the AHJU provided written informed consent.

Data acquisition

Transcriptome data for AHJU stored in the European Genome-phenome Archive (<https://ega-archive.org/>) were available in the EGAD00001004164 dataset. Genome data for AHJU stored in the Genome Sequence Archive for Human (<https://ngdc.cncb.ac.cn/gsa-human/>) were available in the HRA001647 dataset. Data from other cohorts have been previously published and were acquired and preprocessed as described elsewhere.^{19,20} Immune-associated indices, including tumor mutation burden (TMB), tumor neoantigen burden (TNB), microsatellite instability (MSI), and immune subtype, have been previously defined and determined.^{19,20,23}

Screen of hub genes associated with chromatin

We searched for chromatin-associated keywords including “CHROMATIN_ORGANIZATION,” “CHROMATIN_REMODELING,” and “CHROMATIN” in the Gene Ontology (GO) and identified genes for further analysis. Univariate Cox proportional hazard models were used to evaluate the prognostic role of these genes, and the hazard ratios (HRs) and their 95% confidence intervals (CIs) were determined. Then, genes associated with OS were analyzed for protein-protein interactions (PPI) using the search tool for recurring instances of neighboring genes (STRING) (<https://www.string-db.org/>), and the highest linkage hub genes in the network were identified through the Cytoscape plugin CytoHubba.

Whole exome sequencing (WES)

In the AHJU GC cohort, WES was performed on samples from 74 patients, as previously described.²⁰ Briefly, genomic DNA was extracted from tumors and matched with normal tissues. The KAPA Hyper Prep Kit (KAPA Biosystems, USA) was used to prepare the whole-genome library. The Illumina Rapid Capture Extended Exome Kit (Illumina, USA) was used for exome capture. The Illumina HiSeq4000 NGS platform (Illumina, USA) was used to sequence the enriched libraries. Data processing followed published criteria.

Transcriptome sequencing

In the AHJU GC cohort, transcriptome sequencing was conducted on samples from 34 patients, as previously reported.¹⁸ In brief, total RNA was extracted from fresh samples, and ribosomal RNA was depleted later. The KAPA Stranded RNA-seq Kit with RiboErase (KAPA Biosystems, USA) was used to prepare the transcriptome library. After the assessment of library concentration and quality, the Illumina HiSeq4000 NGS platform (Illumina, USA) was used for sequencing. Base calling was applied to generate the sequence reads, which were carried out on bcl2fastq v2.16.0.10 (Illumina, USA) in FASTQ format (Illumina 1.8+ encoding). After quality control using Trimmomatic (version 0.33), STAR (version 2.5.3a) was used to map transcriptomes. RSEM (version 1.3.0) was adopted for isoform- and gene-level quantification.

Immunohistochemistry (IHC) staining

Anti-CHAF1A antibody (ab126625, Abcam, UK) was used for IHC with a 2-step protocol.²⁴ The IHC score was assessed using a semiquantitative method based on the grade categories for the number of stained positive cells and the staining intensity, as previously reported.²⁵ First, we counted the number of positive stained cells in 100 cells in each of 10 selected high power fields (400× magnification) to calculate the percentage of positive stained cells in each section. We classified the percentages 0%, 10–25%, 26–75%, 51–75%, and 76–100% as grade 0, 1, 2, 3, and 4, respectively. Then, staining intensity was also classified as grade 0, 1, 2, and 3 corresponded to no stain, light brown, brown, and dark brown. According to the product of the two grade values, IHC scores were calculated. High expression of the CHAF1A protein was defined as an IHC score ≥ 6 .

Multiple-immunofluorescence (mIF) staining

Following the manufacturer's instructions, mIF staining was performed using the PANO 7-plex IHC kit (Panovue, Beijing, China), with antibodies including anti-panCK (CST4545, Cell Signaling Technology, USA), anti-CD8 (CST70306), anti-HLA-DR (ab92511), anti-CD68 (BX50031, Biolynx, China), anti-S100 (ab52642), and anti-CD56 (CST3576). The reconstruction of section images was based on the Mantra System (PerkinElmer, Waltham, MA, USA). Cells in the images were analyzed and quantified using the inForm image software (PerkinElmer).

Cell lines

Cells of the human GC cell lines (AGS and HGC-27) and the mouse melanoma cell line B16F10 were purchased from the Type Culture Collection of the Chinese Academy of Science (Shanghai, China).

Western blot (WB)

In accordance with standard protocols, WB analysis was conducted using anti-CHAF1A (ab126625), anti-TGF- β 1 (ab215715), anti-pSMAD3 (ab52903), and GAPDH (ab181602) antibodies. In brief, total protein was extracted using lysis buffer containing protease inhibitors, followed by protein quantification. SDS-PAGE gels were used to separate proteins, which were then transferred onto PVDF membranes (Millipore, Bedford, MA, USA). Subsequently, the membranes were blocked with 5% nonfat dry milk and incubated with an anti-CHAF1A antibody overnight at 4°C. Finally, according to standard procedures, immunoblots were probed with ECL detection reagent (Millipore).

Clone selection and cell transfection

For small interfering RNA (siRNA)-mediated CHAF1A silencing (siCHAF1A), the target siRNA sequence of CHAF1A (NM_005483.2) was 5'-CGUUUAAGCGCCUGAAUCU-3'. RNA duplexes were synthesized by RiboBio (Guangzhou, China). Lipofectamine 2000 (Invitrogen) was used to transfect

siRNAs into GC cells. For small hairpin RNA (shRNA)-mediated CHAF1A knockdown (shCHAF1A), the target RNAi sequences, 5'-CCGACTCAATTCCTGTGTA-3' for human cells and 5'-TAGGCTTGAGTACAAAGTT-3' for mouse cells, were synthesized and cloned into the expression vector pGCSIL-green fluorescent protein (GFP) by GeneChem Company (Shanghai, China). The non-target RNAi sequence, 5'-TTCTCCGAACGTGTCACGT-3', was employed to generate the negative control. In accordance with the manufacturer's recommended protocol, lentivirus was added to the cells, and stably transfected cell clones were selected using the limited dilution method. Finally, CHAF1A expression in cells was confirmed by WB.

In vivo experiments

Male C57BL/6 mice, 6–8-week old, were purchased from the Animal Experiment Center of Jiangsu University. For tumor models, each group of B16F10 cells (1×10^6) was subcutaneously injected into C57BL/6 mice. For ICI treatment, tumor-bearing mice were injected via the tail vein with 150 μ l (100 μ g/150 μ l) anti-mouse PD-1 antibody (Bio X Cell Cat# BE0146) or IgG isotype control (Bio X Cell Cat# BE0089) on day 8 after the subcutaneous injection of tumor cells. For tumor volume analysis, all mice were euthanized 20 days after inoculation, and tumors were excised and measured. Tumor volumes were calculated using the following formula: width (mm) \times depth (mm) \times length (mm) \times 0.52. For survival analysis, tumors reaching a maximum subcutaneous tumor size of 550 mm³ were assumed dead and then euthanized. All *in vivo* experiments were randomized in order to evenly distribute the tumor volume among different experimental groups at the beginning of treatment. All experimental procedures were approved by the Institutional Animal Care and Use Committee of Jiangsu University.

Relative tumor proliferation rate

The relative tumor proliferation rate, treatment/control (T/C), was calculated in the vehicle and shCHAF1A groups, respectively. First, the relative tumor volume (RTV) was calculated based on the measurement, using the formula: $RTV = V_t/V_0$, where V_0 is the baseline tumor volume measured after cage administration and V_t is the tumor volume at each measurement. T/C was calculated using the formula: $T/C = RTV_T/RTV_C \times 100\%$; RTV_T is the RTV of the treatment group, and RTV_C is the RTV of the negative control group. A $T/C \leq 40\%$ is considered effective in therapy.²⁶

Statistical analysis

For comparisons between groups, Student's *t*-test, χ^2 test, Fisher's exact probability test, and Mann – Whitney *U* test were used as needed. Survival was analyzed using the KM method and the log-rank test. To define high and low CHAF1A mRNA expression, the optimal cutoff values were determined by the *Survminer* R package according to the association between CHAF1A expression and OS. Correlations between groups were evaluated using the

Pearson correlation coefficient R . To evaluate the predictive power of CHAF1A mRNA expression for the objective response rate (ORR) of patients treated with ICIs, the receiver operating characteristic curve (ROC) and the areas under the ROC curves (AUC) were adopted. A two-sided $p < 0.05$ was perceived as statistically significant. Corrected p values were used as needed. The above analyses were based on SPSS (version 19.0, Chicago, IL), R (version 3.6.1), and R Bioconductor packages.

Results

Eligible patients

The numbers of eligible patients in the ACRG, TCGA, GSE15459, GSE57303, and AHJU cohorts were 300, 415, 192, 70, and 74, respectively (Table. S1). In the AHJU cohort, genome, transcriptome, and IHC data were available for 34, 74, and 48 patients, respectively (Table. S2). For ICI treatment, the numbers of eligible patients in the NCT#02589496, IMvigor210, and AHJU immunotherapy cohorts were 45, 298, and 10, respectively (Table. S3).

Hub genes associated with chromatin in GC

After removing duplicates, a total of 1593 genes in GO terms associated with chromatin were identified and included for screening (Table. S4). Of these, high expression of 30 genes was significantly associated with favorable OS in both the ACRG and TCGA cohorts (Figure 1(a)). They were regarded as candidates to promote the selection of advantageous populations for immunotherapy. After PPI analysis, CHAF1A and UHRF1 were identified as the highest linkage hub genes (Figure 1(b)), while CHAF1A had a more significant prognostic effect than UHRF1 (Figure 1(a)). Survival analysis further confirmed the prognostic role of CHAF1A mRNA expression in the ACRG, TCGA, GSE15459, and GSE57303 cohorts (Figure 1(c)). Moreover, our AHJU data revealed that CHAF1A mRNA expression was a prognostic factor for both disease-free survival (DFS) and OS (Figure 1(d)).

Associations of CHAF1A expression with immune biomarkers in GC

In all the ACRG, AHJU and TCGA cohorts, the MSI GC subtype had significantly higher CHAF1A mRNA expression than the microsatellite stability (MSS) subtype (Figure 2(a)). TMB was also significantly positively correlated with CHAF1A mRNA expression in all three cohorts (Figure 2(b)). Moreover, the expression of most immune effector genes, such as IFNG and GZMB, was significantly positively correlated with CHAF1A mRNA expression (Figure 2(c)). Similar correlations were observed between the expression of CHAF1A and several immune checkpoint genes, such as PD-L1 (CD274) and LAG3 (Fig. S1). Specifically, in the NCT#02589496 cohort, PD-L1 CPS was found to be significantly elevated in the high CHAF1A mRNA expression than in the low (the cutoff value was determined by ROC analysis as shown below) (Figure 2(d)).

To validate the above results, IHC staining of CHAF1A was performed in the AHJU cohort (Table. S2 and Figure 2(e)). The MSI GC subtype also had significantly higher CHAF1A protein expression than the MSS subtype (Figure 2(f)). TMB was also significantly positively correlated with the IHC score of CHAF1A ($R = 0.48$, $p < 0.001$; Figure 2(g)). Furthermore, the mRNA expression of most immune effector genes was significantly positively correlated with the CHAF1A IHC score (Figure 2(h)).

Association of CHAF1A expression with immune infiltration in GC

The C2 GC subtype of TCGA, indicating an IFN-gamma dominant phenotype, had the highest mRNA expression of CHAF1A among the immune subtypes (Figure 3(a)). The abundance of infiltrating immune cells in the tumor microenvironment (TME) was evaluated using the xCell algorithm based on transcriptome data.²⁷ CHAF1A mRNA expression was significantly positively correlated with the abundance of Th1 cells ($R = 0.73$, 0.86 , and 0.61 , respectively) and macrophages M1, but was significantly negatively correlated with the abundance of fibroblasts ($R = -0.49$, -0.47 , and -0.45 , respectively), in all the ACRG, AHJU, and TCGA cohorts (Figure 3(b)). In addition, CHAF1A mRNA expression was significantly positively correlated with the abundance of NK cells in both the ACRG and TCGA cohorts (Figure 3(b)).

mIF results were available for eight AHJU patients with their transcriptome data (Figure 3(c)). The cells in the invasive margin and tumor parenchyma were quantified separately. In the tumor parenchyma, CHAF1A mRNA expression was positively correlated with the densities of NK cells (including CD56bright and CD56dim subtypes; $R = 0.62$) and macrophages M1 ($R = 0.69$), but was negatively correlated with the density of macrophages M2 ($R = -0.29$; Figure 3(d)). However, the significance of these results was limited by the small sample size. Next, the effective infiltration score (EIS) was defined as the number of immune cells in the tumor parenchyma divided by the total number of immune cells in TME.¹⁸ CHAF1A mRNA expression was positively correlated with the EIS of NK cells ($R = 0.52$) and macrophages M1 ($R = 0.24$) and negatively correlated with the EIS of macrophages M2 ($R = -0.81$, $p < 0.05$; Figure 3(e)).

Association of CHAF1A expression with the effect of ICIs in GC

In the NCT#02589496 cohort, GC patients who responded to second-line treatment with pembrolizumab had significantly higher CHAF1A mRNA expression than those who did not respond ($p = 0.031$; Figure 4(a)). ROC analysis showed that the AUC for the prediction of CHAF1A mRNA expression to response was 0.712 (Figure 4(b)). Based on the optimal threshold of CHAF1A mRNA expression for the maximum ROC curve values, the patients were dichotomized into high- and low-expression subgroups. The high-expression subgroup presented a significantly higher ORR than the low-expression subgroup (47.3% vs. 11.5%, $p = 0.007$; Figure 4(c)).

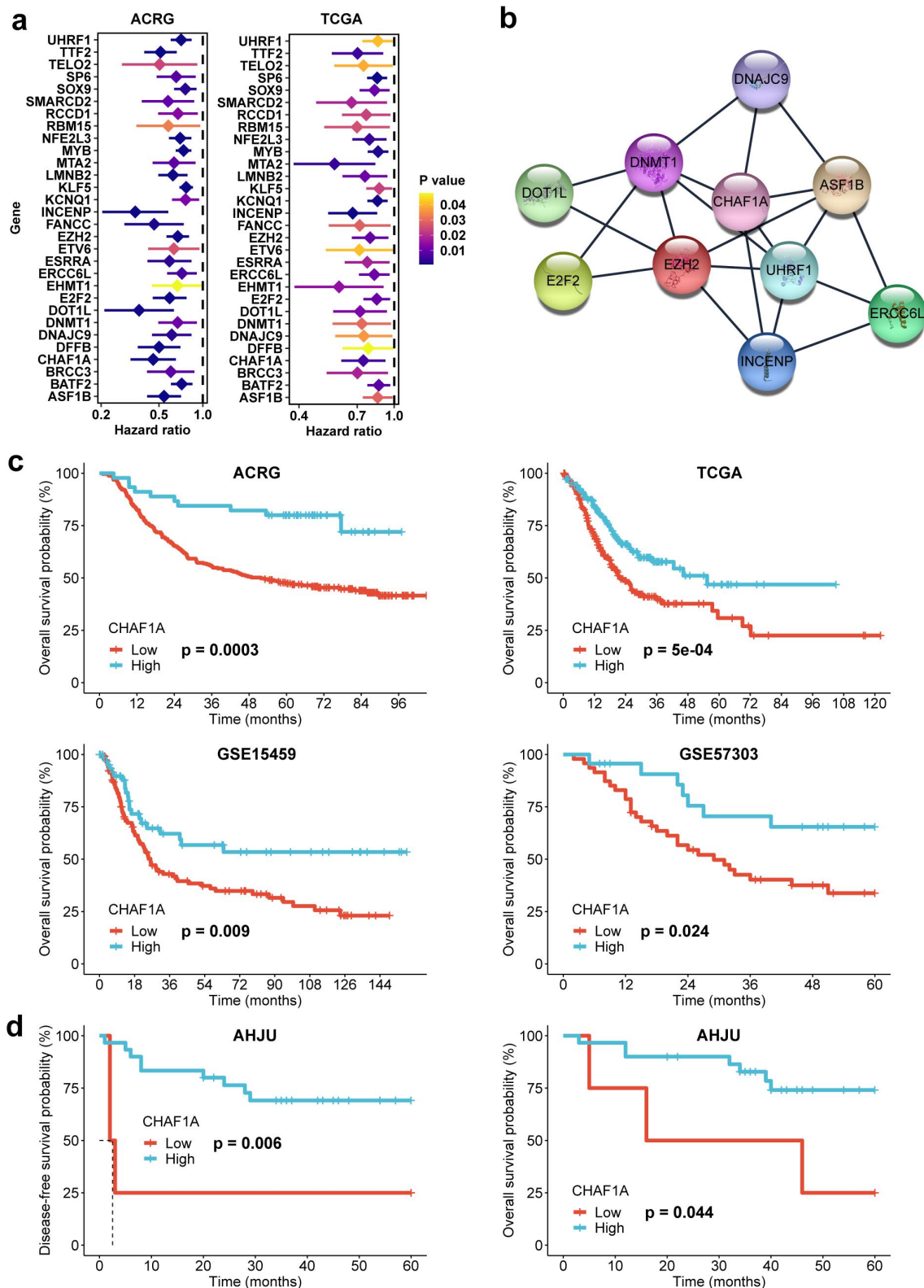


Figure 1. Hub gene selection. (a) genes associated with chromatin and favorable prognosis in GC from the ACRG and TCGA cohorts. (b) CHAF1A and UHRF1 were identified as the highest linkage hub genes in the protein-protein interaction analysis. (c) overall survival (OS) analysis for CHAF1A in GC from the ACRG, TCGA, GSE15459, and GSE57303 cohorts. (d) OS and disease-free survival analysis for CHAF1A in the AHJU cohort. GC: gastric cancer; ACRG: Asian cancer Research Group; AHJU: Affiliated Hospital of Jiangsu University; TCGA: the cancer genome atlas.

Importantly, the association between CHAF1A expression and response to pembrolizumab was not limited by TMB or MSI status. High CHAF1A expression showed better ORR than low expression in both the MSI (100%

vs. 66.7%) and microsatellite stable (MSS; 37.5% vs. 4.3%) subsets, and both the high TMB (83.3% vs. 40%) and low TMB (30.8% vs. 4.8%) subsets (Table 1). No response was observed in patients with a PD-L1 CPS of < 1. However,

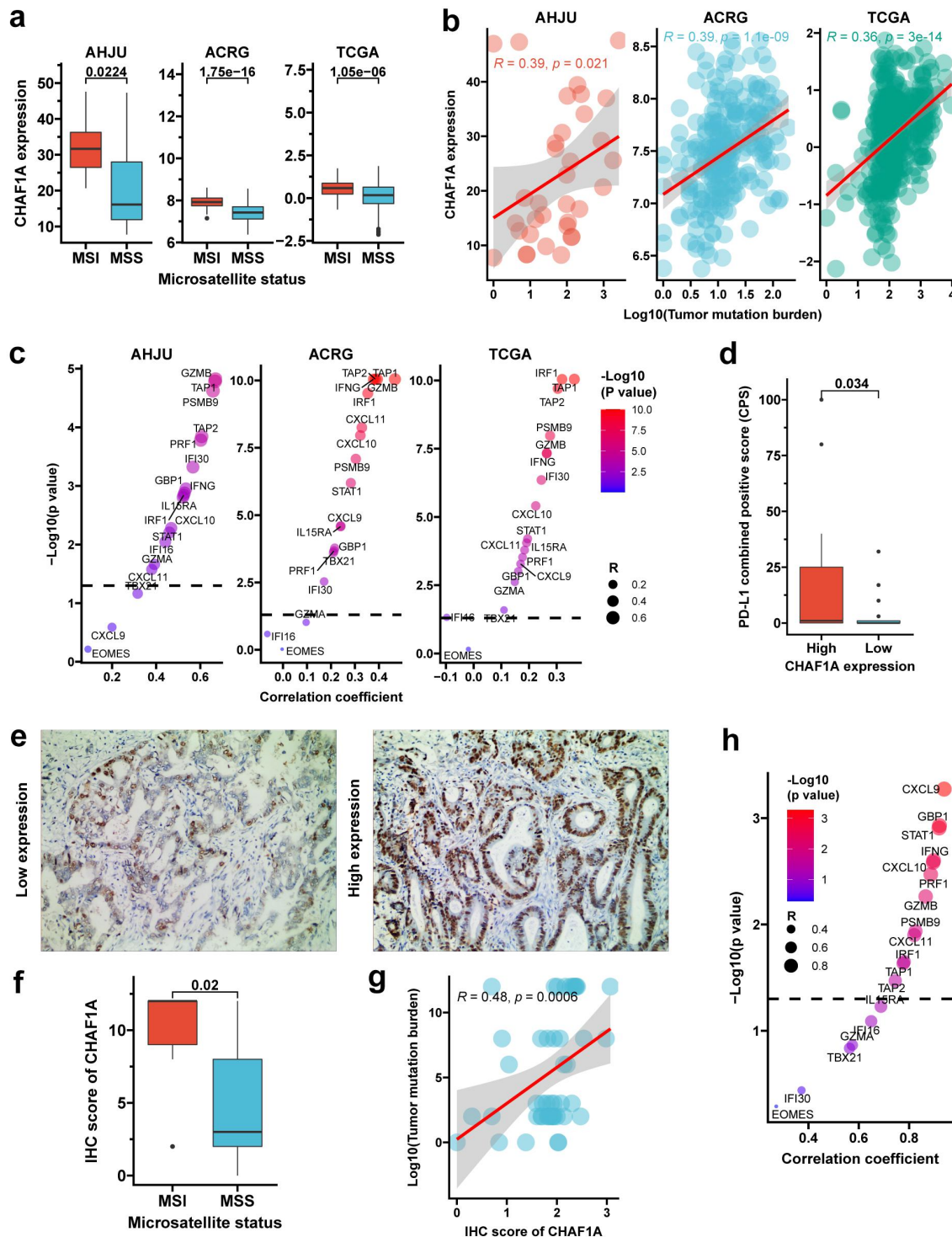


Figure 2. CHAF1A expression and immune biomarkers. (a) CHAF1A mRNA expression by MSI status. (b) correlation of CHAF1A mRNA expression with tumor mutation burden (TMB). (c) correlation between mRNA expressions of CHAF1A and immune effector genes. (d) PD-L1 combined positive score by CHAF1A expression in the NCT#02589496 cohort. (e) typical micrograph of CHAF1A IHC staining in tumors, at 200×magnification. (f) IHC score of CHAF1A by MSI status. (g) correlation between TMB and CHAF1A IHC score. (h) correlation between CHAF1A IHC score and the mRNA expression of immune effector genes. GC: gastric cancer; MSI: microsatellite instability; MSS: microsatellite stability; IHC: immunohistochemistry; ACRG: Asian cancer Research Group; AHJU: Affiliated Hospital of Jiangsu University; TCGA: the cancer genome atlas.

high CHAF1A expression still indicated a better ORR in the CPS ≥ 1 subgroup (69.2% vs. 22.2%; Table 1).

In the AHJU immunotherapy cohort, GC patients who responded to the first-line combination of chemotherapy with anti-PD-1 antibodies had a significantly higher IHC score for CHAF1A protein than those who did not respond

($p = 0.03$; Figure 4(d)). The AUC for the prediction of the CHAF1A IHC score to response was 0.976 (Figure 4(e)). The high-expression subgroup of CHAF1A protein (IHC score ≥ 6) also showed a higher ORR than the low-expression subgroup (83.3% vs. 25%, $p = 0.065$; Figure 4(f)). Furthermore, patients with high expression of

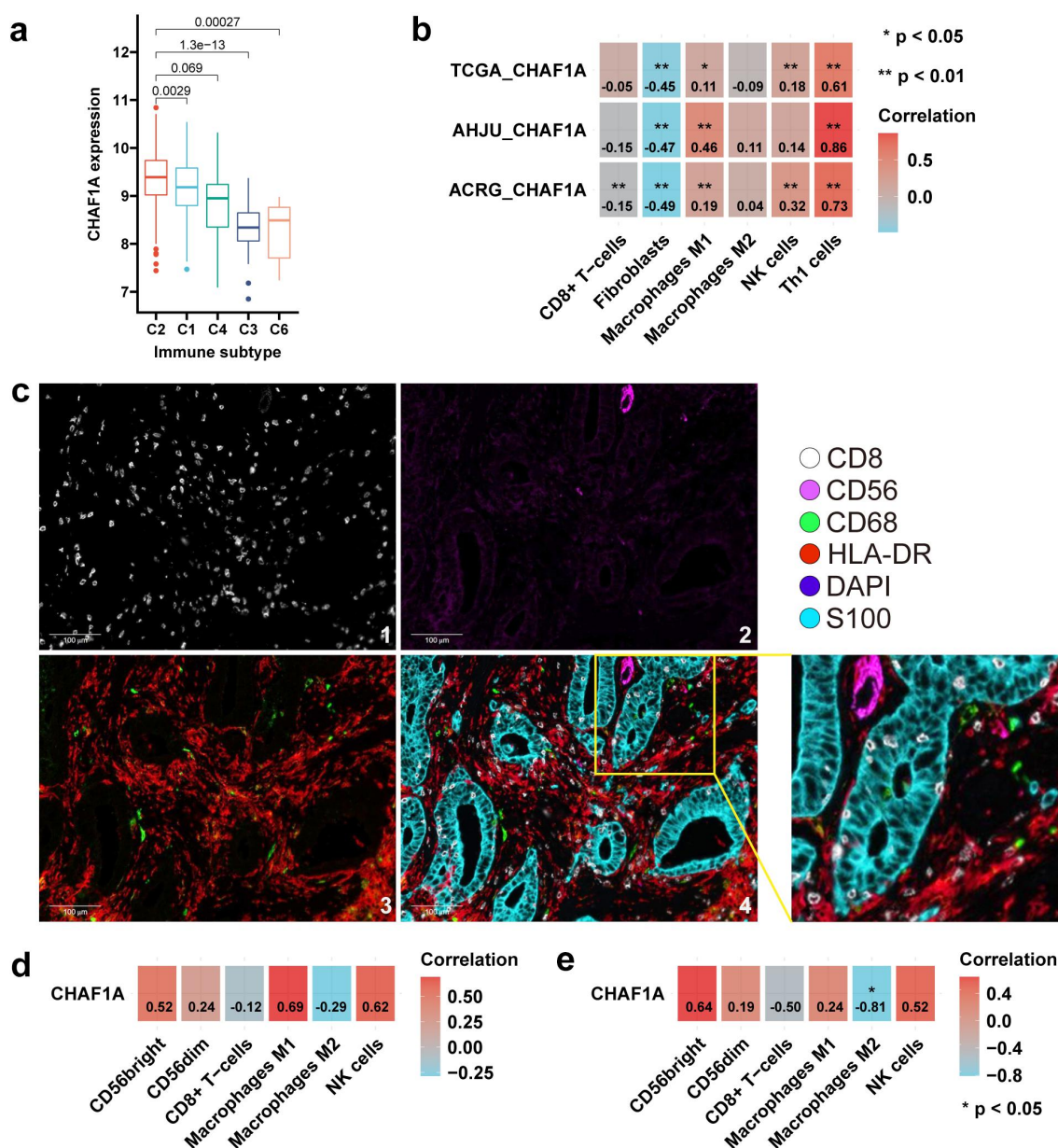


Figure 3. CHAF1A expression and immune infiltration. (a) CHAF1A mRNA expression in GC by immune phenotype in TCGA. (b) correlation of CHAF1A mRNA expression with the abundance of infiltrating immune cells. (c) typically microscopic image of surface biomarkers of immune cells by multiplexed immunohistochemistry staining in AHJU. 1: CD8; 2: CD56; 3: CD68 (green) and HLA-DR (red); 4: the reconstructed image for all surface biomarkers. (d) correlation of CHAF1A mRNA expression with the densities of immune cells in the tumor parenchyma. (e) correlation of CHAF1A mRNA expression with the effective infiltration score of immune cells. GC: gastric cancer; ACRG: Asian cancer Research Group; AHJU: Affiliated Hospital of Jiangsu University; TCGA: the cancer genome atlas.

CHAF1A protein had better PFS ($p = 0.044$; Figure 4(g)) and OS ($p = 0.075$; Figure 4(h)) than those with low expression.

CHAF1A expression as an immune biomarker in other tumors

Pan-tumor analysis was performed for CHAF1A in TCGA. CHAF1A mRNA was overexpressed in tumor tissues compared to normal tissues in most tumor types (Fig. S2A). The MSI subtype had significantly higher CHAF1A mRNA expression than the MSS subtype in colorectal cancer and uterine corpus endometrial carcinoma, both of which have a higher MSI frequency than other tumors (Fig. S2B). TMB (Fig. S2C),

and TNB (Fig. S2D) were positively correlated with CHAF1A mRNA expression in most tumor types, whereas a contrasting result was observed in thymoma. For immune infiltration, CHAF1A mRNA expression was significantly positively correlated with the abundance of Th1 cells in all tumor types but was negatively correlated with the abundance of fibroblasts and macrophages M2 in most tumor types (Fig. S3).

In the IMvigor210 cohort, patients with mUC who responded to atezolizumab exhibited significantly higher CHAF1A mRNA expression than those who did not respond (Figure 4(i)). The AUC for the prediction of CHAF1A expression to response was 0.644 (Figure 4(j)). High CHAF1A expression resulted in a better ORR than low expression (49% vs. 17.4%, $p = 0.001$; Figure 4(k)). Furthermore, StromalScore,

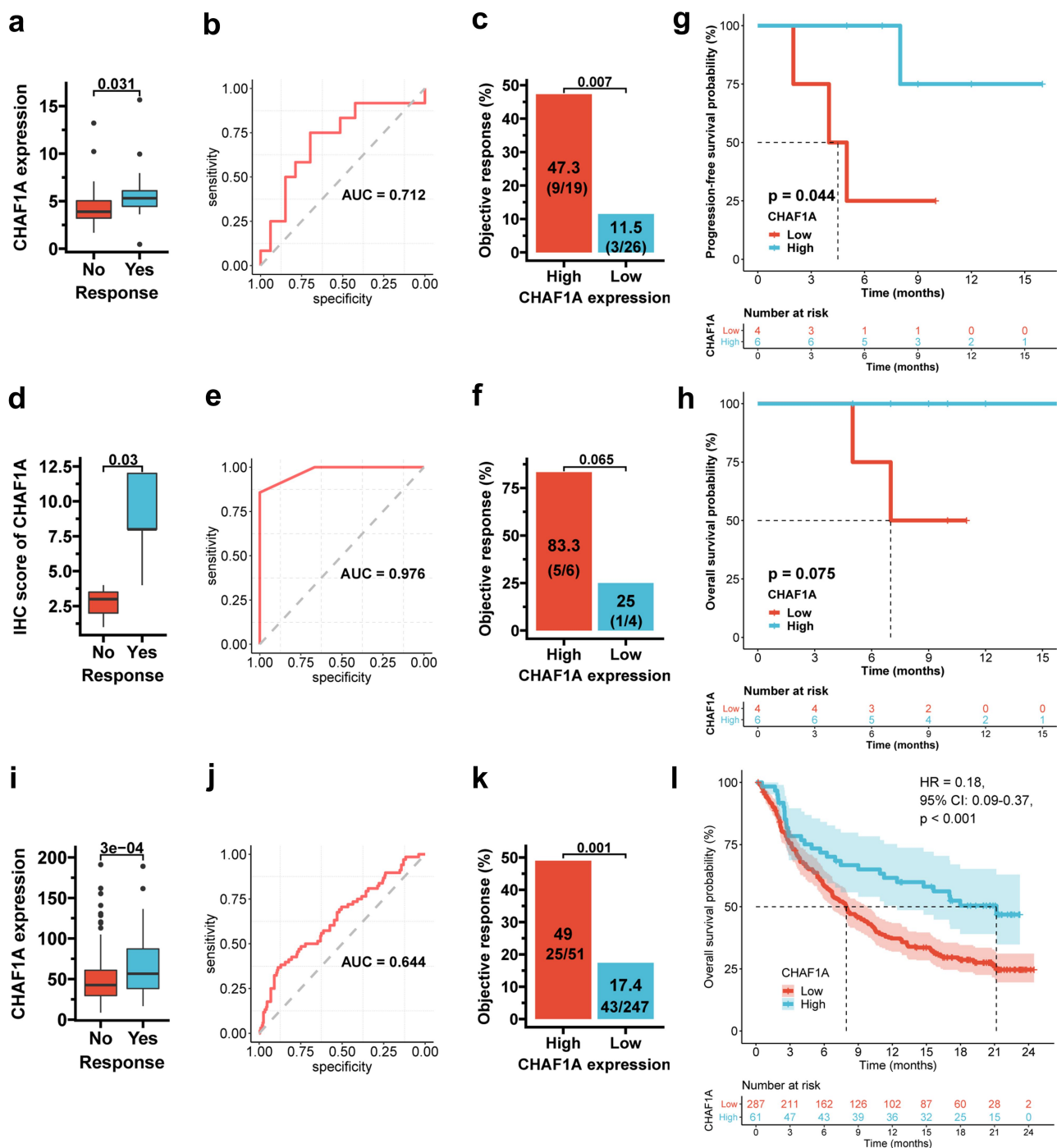


Figure 4. CHAF1A expression and immunotherapy outcome. (a) CHAF1A mRNA expression by response status in the NCT#02589496 cohort. (b) the ROC curve for response prediction by CHAF1A mRNA expression. (c) objective response rate (ORR) by CHAF1A expression level. (d) the IHC score of CHAF1A protein by response in the AHJU immunotherapy cohort. (e) the ROC curve for response prediction by CHAF1A IHC score. (f) ORR by CHAF1A protein expression. (g,h) progression-free survival (g) and overall survival (h) by CHAF1A protein expression. (i) CHAF1A mRNA expression by response status in the IMvigor210 cohort. (j) the ROC curve for response prediction by CHAF1A mRNA expression. (k) objective response rate by CHAF1A expression level. (l) overall survival by CHAF1A expression level. GC: gastric cancer; IHC: Immunohistochemistry; AHJU: Affiliated Hospital of Jiangsu University; ROC: receiver operating characteristic curve; AUC: the areas under the ROC curves. HR: hazard ratio; CI: confidence interval.

ImmuneScore, and ESTIMATEScore may impact ICI efficacy and were calculated.²⁸ In this cohort, the immune phenotype, TMB, and TNB were available, and PD-L1 expression on immune cells (IC) and tumor cells (TC) was assessed and scored as IC0/TC0 (<1%), IC1/TC1 ($\geq 1\%$ and <5%), or IC2/TC2 ($\geq 5\%$). The predictive ability of CHAF1A expression for

response was not affected by these indexes or by sampling locations (primary lesion or metastasis), and the response superiority associated with high CHAF1A expression existed in all stratifications (Table 1 and S5). Furthermore, patients with high CHAF1A expression displayed significantly better OS than those with low expression (HR = 0.18, 95% CI: 0.09–

Table 1. Immunotherapy response by CHAF1A mRNA expression.

Biomarker (response rate, %)	Response	CHAF1A expression		P value
		Low (%)	High (%)	
In the NCT#02589496 cohort				
Microsatellite status				
MSS (17.9)	No	22 (95.7)	10 (62.5)	0.008
	Yes	1 (4.3)	6 (37.5)	
MSI (83.3)	No	1 (33.3)	0 (0.0)	0.273
	Yes	2 (66.7)	3 (100.0)	
Tumor mutation burden*				
Low (14.7)	No	20 (95.2)	9 (69.2)	0.037
	Yes	1 (4.8)	4 (30.8)	
High (63.6)	No	3 (60.0)	1 (16.7)	0.137
	Yes	2 (40.0)	5 (83.3)	
PD-L1 combined positive score (CPS)				
<1 (0)	No	13 (100.0)	6 (100.0)	-
≥1 (50)	No	7 (77.8)	4 (30.8)	
	Yes	2 (22.2)	9 (69.2)	
In the IMvigor210 cohort				
Tumor mutation burden*				
Low (16.4)	No	166 (86.0)	17 (65.4)	0.008
	Yes	27 (14.0)	9 (34.6)	
High (40.5)	No	38 (70.4)	9 (36.0)	0.004
	Yes	16 (29.6)	16 (64.0)	
Tumor neoantigen burden*				
Low (14.7)	No	184 (88.0)	19 (65.5)	0.001
	Yes	25 (12.0)	10 (34.5)	
High (55.0)	No	20 (52.6)	7 (31.8)	0.118
	Yes	18 (47.4)	15 (68.2)	
PD-L1 expression on immune cells (IC)				
IC0 (15.7)	No	62 (89.9)	8 (57.1)	0.002
	Yes	7 (10.1)	6 (42.9)	
IC1 (17.9)	No	82 (86.3)	10 (58.8)	0.006
	Yes	13 (13.7)	7 (41.2)	
IC2 (34.3)	No	59 (72.0)	8 (40.0)	0.007
	Yes	23 (28.0)	12 (60.0)	
PD-L1 expression on tumor cells (TC)				
TC0 (22.3)	No	163 (82.3)	22 (55.0)	<0.001
	Yes	35 (17.7)	18 (45.0)	
TC1 (29.4)	No	10 (100.0)	2 (28.6)	0.001
	Yes	0 (0.0)	5 (71.4)	
TC2 (23.8)	No	30 (78.9)	2 (50.0)	0.196
	Yes	8 (21.1)	2 (50.0)	
Immune phenotype				
Inflamed (30.6)	No	36 (76.6)	7 (46.7)	0.029
	Yes	11 (23.4)	8 (53.3)	
Desert (20.3)	No	47 (83.9)	8 (61.5)	0.071
	Yes	9 (16.1)	5 (38.5)	
Excluded (24.8)	No	78 (80.4)	7 (43.8)	0.002
	Yes	19 (19.6)	9 (56.2)	
StromalScore*				
Low (28.3)	No	95 (79.8)	24 (51.1)	<0.001
	Yes	24 (20.2)	23 (48.9)	
High (15.9)	No	109 (85.2)	2 (50.0)	0.058
	Yes	19 (14.8)	2 (50.0)	
ImmuneScore*				
Low (21.4)	No	152 (84.0)	24 (55.8)	<0.001
	Yes	29 (16.0)	19 (44.2)	
High (27.0)	No	52 (78.8)	2 (25.0)	0.004
	Yes	14 (21.2)	6 (75.0)	
ESTIMATEScore*				
Low (27.3)	No	88 (80.0)	21 (52.5)	0.001
	Yes	22 (20.0)	19 (47.5)	
High (18.2)	No	116 (84.7)	5 (45.5)	0.001
	Yes	21 (15.3)	6 (54.5)	

*Based on the optimal threshold of these biomarkers for the maximum ROC curve values, the patients were dichotomized into high and low subgroups.

0.37, $p < 0.001$; Figure 4(l)). Such OS superiority associated with high CHAF1A expression also existed in all stratifications by above indexes (Fig. S4 and S5).

CHAF1A knockdown and anti-PD-1 effect in vivo

CHAF1A knockdown was previously reported to inhibit cell proliferation in tumors, including GC,^{16,29,30} but our results indicated that low CHAF1A expression was harmful to immunotherapy. Thus, the impact of CHAF1A knockdown (Figure 5(a)) on the anti-PD-1 effect was investigated in B16F10 tumors of immunocompetent C57bl/6 mice (Figure 5(b)). Compared with the IgG isotype control, anti-PD-1 antibody significantly inhibited tumor growth in the vehicle group (Figure 5C). This result was also observed in the shCHAF1A group, while the ability of the anti-PD-1 antibody to shrink tumors was obviously impaired by CHAF1A knockdown (Figure 5(d) and S6 [all curves overlaid]), which was validated by the comparison between the vehicle and shCHAF1A groups for tumor volume reduction induced by the anti-PD-1 antibody especially after post-treatment day 9 (Figure 5(e)). Furthermore, T/C was used to evaluate the relative tumor proliferation, which was higher in the shCHAF1A group than that in the vehicle group, after post-treatment day 7, especially on day 9 (Figure 5(f)). The mean T/C at the endpoint time, post-treatment day 13, in the shCHAF1A group was 42.8%, which failed to reach the effective threshold of 40%, which was 34.3% in the vehicle group (Figure 5(f)). These findings again indicate that CHAF1A knockdown damages the effect of the anti-PD-1 antibody. Moreover, in the survival experiment, although the anti-PD-1 antibody significantly improved the post-treatment survival of animals compared with the IgG isotype control in both the vehicle and shCHAF1A groups, the survival benefit obviously decreased in the shCHAF1A group, the prolonged median survival were 5 and 2 days in these two groups, respectively (Figure 5(g)).

Association of CHAF1A with the inhibition of TGF- β signaling

Differentially expressed genes between the high and low subgroups (upper and lower quartiles) of CHAF1A mRNA expression were determined in ACRG (Figs. S7A and S7B). Gene set enrichment analysis (GSEA) based on GO biological processes (BP) was performed (Fig. S7C). GO BP terms involving tumor development and immune inhibition were enriched in the low expression group, such as angiogenesis, epithelial to mesenchymal transition, TGF- β receptor signaling pathway, and Ras protein signal transduction. The GO BP terms involving immune response and genetic fidelity were enriched in the high expression group, such as defense response to viruses, interaction with hosts, chromatin assembly or disassembly, DNA repair, DNA replication, and cell cycle checkpoint. Specifically, genes involved in TGF- β -associated signaling were generally down-regulated in the high-expression group (Figure 6(a)).

Because TGF- β signaling has been proven to inhibit anti-tumor immune responses and cause tumor resistance to immunotherapy,^{22,31} we further investigated the potential inhibition of CHAF1A on TGF- β signaling. First, TGF- β scoring was conducted based on the transcriptome and several well-established gene signatures using the PGSEA R package.¹⁷ In both ACRG and TCGA, CHAF1A mRNA

expression was significantly negatively correlated with all TGF- β scores (Figure 6(b)). Next, siCHAF1A-treated AGS and HGC-27 cells were generated. CHAF1A siRNA significantly promoted the expression of TGF- β 1 and its downstream effector, phosphorylated SMAD3 (pSMAD3) (Figure 6(c,d)). A TGF- β receptor inhibitor (TGF β RI), SB-431542 (MCE, USA), was used to treat shCHAF1A-treated AGS and HGC-27 cells. The upregulation of TGF- β 1 and pSMAD3 through CHAF1A knockdown was significantly inhibited by TGF β RI (Figure 6(e,f)).

Discussion

Recently, epigenetic alterations are found to play a critical role in tumor immune escape. Epidrugs against epigenetic alterations, such as histone deacetylase (HDAC) inhibitors, which can activate the anti-tumor immune response, had been studied in the combinations with immunotherapy.^{32,33} Meanwhile, genes that compose or regulate chromatin have demonstrated a promising prospect for guiding cancer therapy as biomarkers.^{14,15} In this study, we screened hub genes associated with chromatin in GC and found that CHAF1A could be

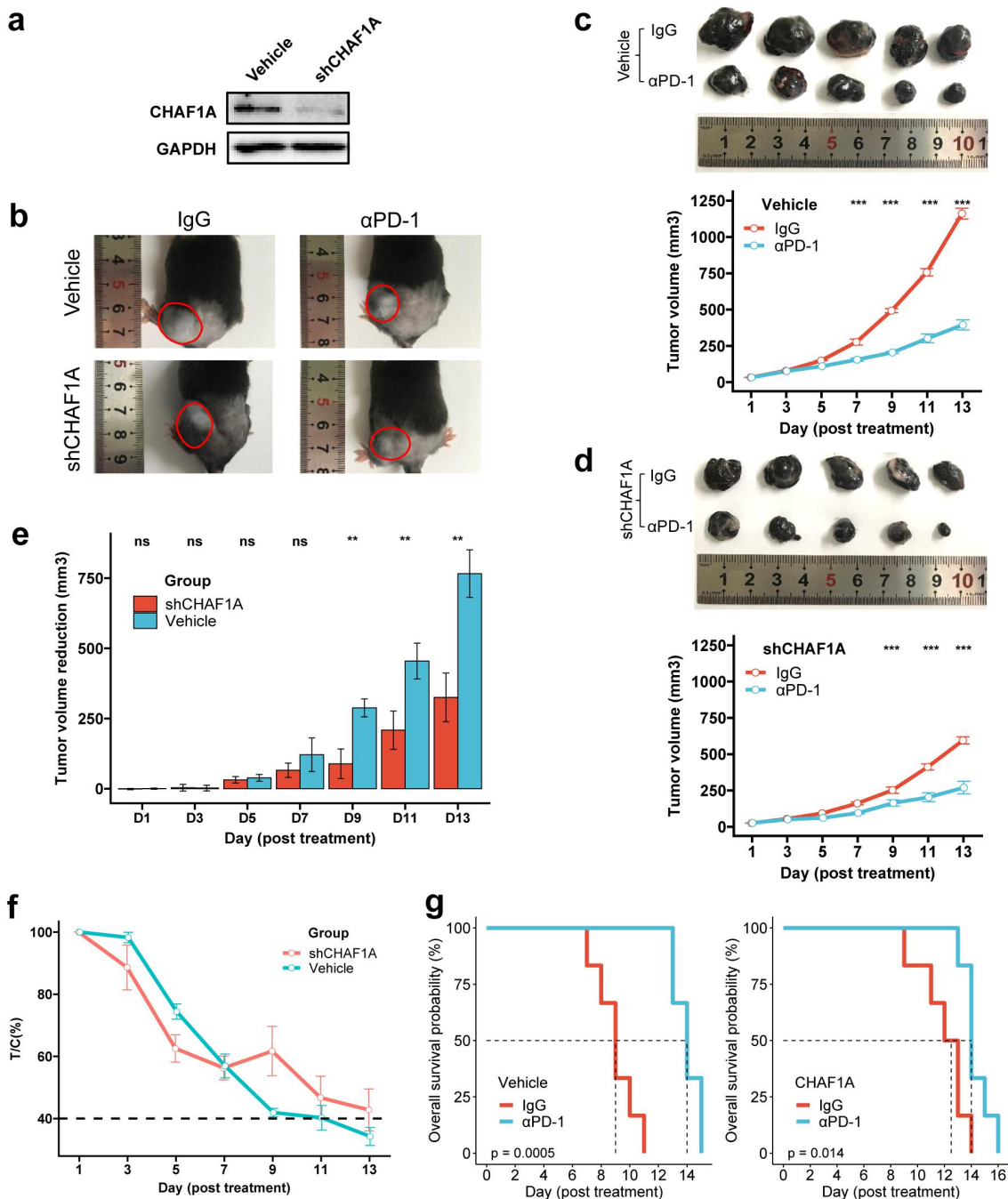


Figure 5. CHAF1A knockdown and anti-PD-1 effect. (a) CHAF1A knockdown in B16F10 cells. (b) tumors *in vivo* on the 20th day after subcutaneous injection of B16F10 cells treated by vehicle and shCHAF1A into C57bl/6 mice. (c,d) The inhibited effects of anti-PD-1 antibody on tumor growth and the tumor growth curves in the vehicle (c) and shCHAF1A (d) groups, respectively. (e) tumor volume reduction induced by anti-PD-1 antibody between the vehicle and shCHAF1A groups. (f) The relative tumor proliferation rate T/C. (g) survival curves of mice in the vehicle and shCHAF1A groups, respectively.

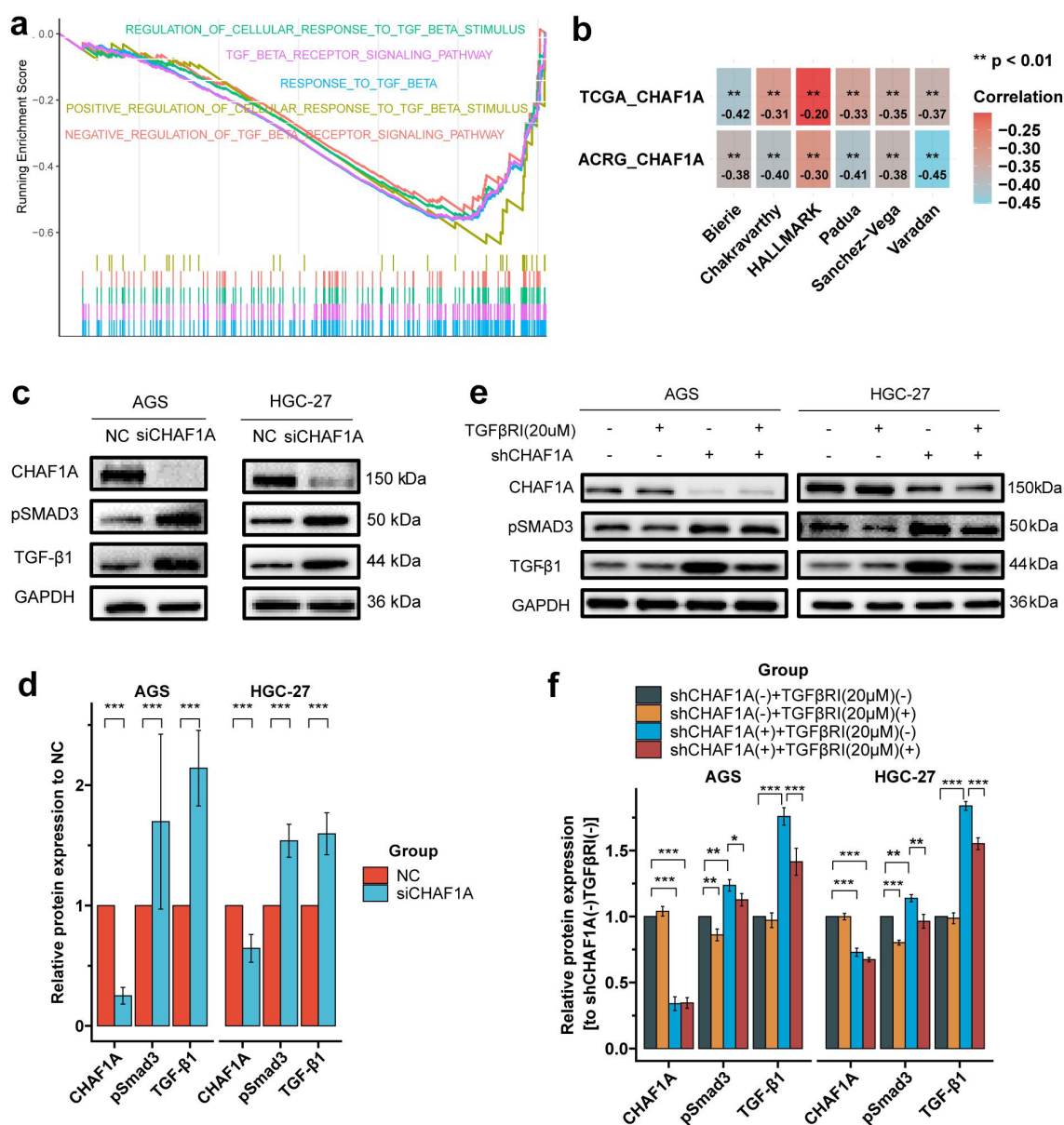


Figure 6. CHAF1A expression and TGF- β signaling. (a) Gene set enrichment analysis by CHAF1A expression levels indicated that signaling associated with TGF- β were down-regulated in the high expression group. (b) correlation of CHAF1A mRNA expression with TGF- β scores (signature authors are shown) based on transcriptome. (c) CHAF1A siRNA (siCHAF1A) up-regulates the expressions of TGF- β 1 and phosphorylated SMAD3 (pSMAD3). (d) quantization of grayscale values in figure C. (e) the TGF- β receptor inhibitor (TGF β RI) SB-431542 inhibits the up-regulation of TGF- β 1 and pSMAD3 by CHAF1A shRNA (shCHAF1A). (f) quantization of grayscale values in figure e. ACRG: Asian Cancer Research Group; TCGA: the Cancer genome atlas.

a candidate biomarker for immunotherapy with ICIs. Importantly, the role of CHAF1A spanned across tumor types and subtypes defined by other biomarkers such as MSI, TMB, PD-L1, immune phenotype, or immune-associated scores. Interestingly, CHAF1A was previously reported as an oncogene that promotes GC growth¹⁶; its inhibition, however, impeded anti-PD-1 therapy *in vivo* potentially through the activation of TGF- β signaling. These results will contribute to the development of precise immunotherapies.

CHAF1A, encoding protein p150, is the largest subunit of human chromatin assembly factor 1 (CAF-1), which is a three-subunit protein complex including p150, p60, and p48.³⁴ As a histone chaperone, CAF-1 is crucial for nucleosome assembly, chromatin silencing, and heterochromatin integrity.³⁵

Through a leading role in CAF-1 functions, CHAF1A is involved in gene expression and regulation, DNA replication and repair, cell differentiation and death, cell cycle and proliferation, and so on.^{36,37} However, the role of CHAF1A in immune regulation remains unclear. In this study, CHAF1A was overexpressed in tumors with MSI, high TMB, and high TNB, characterized by dynamic anti-tumor immune reactions. CHAF1A was also positively correlated with the expression of immune effector genes and anti-tumor immune infiltration. These results indicate a role for CHAF1A in the immune response, which was further stressed by the potentially inhibition of CHAF1A on TGF- β signaling. It is well known that TGF- β signaling is the key driver for immune inhibition and immune cell exclusion, which causes resistance to

immunotherapy.^{22,31} Thus, the close relationship between CHAF1A expression and therapeutic response and prognosis of patients treated with ICIs may be partly explained.

Currently, the most commonly used predictive biomarkers for ICI efficacy include MSI status, TMB level, and PD-L1 expression. However, the advantageous population defined by these biomarkers still has many non-responding patients, while the corresponding disadvantageous population still presents a certain efficacy. In this study, the combination of these biomarkers with CHAF1A expression significantly improved patient selection. The redefined advantageous population obtained substantially better ORR; meanwhile, patients with response potential among the previously disadvantaged population have been largely identified. Similar results were observed in the combination of CHAF1A with immune phenotype and signature scoring based on the transcriptome. Moreover, the CHAF1A expression assay among different metastatic locations showed its robustness for the prediction of ICI efficacy in the IMvigor210 cohort. These findings suggest that CHAF1A is a key upstream modulator of the immune response and may act as a favorable chaperone of existing biomarkers to predict immunotherapy efficacy.

It would be interesting to find an unexpected dual role for CHAF1A in tumorigenesis and anti-tumor immunoreaction. Previously, CHAF1A was found to be oncogenic and growth-promoting in many tumors, such as colon cancer,²⁹ neuroblastoma,³⁰ breast cancer,³⁸ and GC.¹⁶ In this study, CHAF1A knockdown still inhibited tumor growth *in vivo*, but it impaired the effect of anti-PD-1 antibody to reduce tumor size and prolong the survival of tumor-carrying mice. Actually, genes with double-sided roles have been widely reported, whose specific functions are determined by disease development, the local microenvironment, mutations or functional status of other genes, and other factors.^{39–42} Nonetheless, to our knowledge, this is the first study to reveal an association between an oncogene and an active anti-tumor immune response. Beyond the potential TGF- β signaling suppression, another possible explanation is that CHAF1A overexpression induces hyperactive DNA replication, as indicated by previous evidences^{35,37} and our GSEA. It is well-known that increased replication stress in tumor cells activates an intrinsic immune response based on cGAS-STING signaling through replication-stress-induced cytosolic DNA accumulation.⁴³ In addition, it has been established that replication stress is a major contributor to genome instability in cancer cells,⁴⁴ which may explain the close relationship between CHAF1A overexpression and MSI and high TMB.

This study had several limitations. First, the association of CHAF1A expression with ICI efficacy needs further validation in prospective studies with larger samples. Second, the molecular mechanisms of CHAF1A to potentially inhibit TGF- β signaling and other potential mechanisms of CHAF1A to activate the immune response require further investigations. Especially, the impact of TGF inhibitors on the role of CHAF1A knockdown needs to be explored. Third, we preferred to built an immunotherapy model for GC instead of melanoma, while our attempts failed due to technical problems. Moreover, cell lines chosen in this study may be controversial, because of the different responsiveness of AGS cells

to CHAF1A knockdown predicted by databases, and the heterogeneous B16F10 responsiveness to ICIs reported by studies.^{45,46} Furthermore, both mRNA and protein expression of CHAF1A can predict ICI efficacy, but the optimal detection methods and standards still need to be established. Finally, an inconsistent prognostic role of CHAF1A has been previously reported in GC and other tumors,^{16,29,38} although multiple pieces of evidence for its favorable role in prognosis from several cohorts were provided in this study.

In conclusion, CHAF1A may be a novel biomarker for predicting immunotherapy efficacy in GC and other tumors. Importantly, the predictive role of CHAF1A was independent of classic biomarkers such as MSI, TMB, and PD-L1, even if they were closely related, which highlights the key role of CHAF1A in upstream signaling of the immune response and provides the potential to improve patient selection in immunotherapy. Further validation and mechanistic studies are needed.

Availability of data and material

All data relevant to the study that are not in the article and supplementary material are available from the corresponding author on reasonable request.

Disclosure statement

No potential conflict of interest was reported by the author(s).

Funding

The study was funded by Innovation Funds From The Natural Science Foundation of Jiangsu Province [BK20231252], Key Medical Research Projects of Jiangsu Provincial Health Commission [K2023026], Chinese Society Of Clinical Oncology Youth Committee [Y-Young2021-01074], China Postdoctoral Science Foundation [2021M693272], Science and Technology Planning Social Development Project of Zhenjiang City [SH2022047], and Medical Education Collaborative Innovation Fund from Jiangsu University [JDY2022003].

ORCID

Deqiang Wang  <http://orcid.org/0000-0002-8411-312X>

Human rights statement and informed consent:

The study was approved by relevant regulatory and independent ethics committees of the Affiliated Hospital of Jiangsu University and Jiangsu University and done in accordance with the Declaration of Helsinki and the International Conference on Harmonization Good Clinical Practice guidelines. All patients provided written, informed consent before study entry.

References

1. Wang Y, Zhang H, Liu C, Wang Z, Wu W, Zhang N, Zhang L, Hu J, Luo P, Zhang J. et al. Immune checkpoint modulators in cancer immunotherapy: recent advances and emerging concepts. *J Hematol Oncol.* 2022;15(1):111. doi:10.1186/s13045-022-01325-0.
2. Janjigian YY, Shitara K, Moehler M, Garrido M, Salman P, Shen L, Wyrwicz L, Yamaguchi K, Skoczytas T, Campos Bragagnoli A. et al.

- First-line nivolumab plus chemotherapy versus chemotherapy alone for advanced gastric, gastro-oesophageal junction, and oesophageal adenocarcinoma (CheckMate 649): a randomised, open-label, phase 3 trial. *Lancet*. 2021;398(10294):27–40. doi:10.1016/S0140-6736(21)00797-2.
3. Zhao JJ, Yap D, Chan YH, Tan B, Teo CB, Syn NL, Smyth EC, Soon YY, Sundar R. Low programmed death-ligand 1-expressing subgroup outcomes of first-line immune checkpoint inhibitors in gastric or esophageal adenocarcinoma. *J Clin Oncol*. 2022;40(4):392–402. doi:10.1200/JCO.21.01862.
 4. Shitara K, Van Cutsem E, Bang YJ, Fuchs C, Wyrwicz L, Lee KW, Kudaba I, Garrido M, Chung HC, Lee J. et al. Efficacy and safety of Pembrolizumab or Pembrolizumab plus chemotherapy vs chemotherapy alone for patients with first-line, advanced gastric cancer: the KEYNOTE-062 phase 3 randomized clinical trial. *JAMA Oncol*. 2020;6(10):1571–1580. doi:10.1001/jamaoncol.2020.3370.
 5. Hagi T, Kurokawa Y, Kawabata R, Omori T, Matsuyama J, Fujitani K, Hirao M, Akamaru Y, Takahashi T, Yamasaki M. et al. Multicentre biomarker cohort study on the efficacy of nivolumab treatment for gastric cancer. *Br J Cancer*. 2020;123(6):965–972. doi:10.1038/s41416-020-0975-7.
 6. Narita Y, Sasaki E, Masuishi T, Taniguchi H, Kadowaki S, Ito S, Yatabe Y, Muro K. PD-L1 immunohistochemistry comparison of 22C3 and 28-8 assays for gastric cancer. *J Gastrointest Oncol*. 2021;12(6):2696–2705. doi:10.21037/jgo-21-505.
 7. Yamashita K, Iwatsuki M, Harada K, Koga Y, Kiyozumi Y, Eto K, Hiyoshi Y, Ishimoto T, Iwagami S, Baba Y. et al. Can PD-L1 expression evaluated by biopsy sample accurately reflect its expression in the whole tumour in gastric cancer? *Br J Cancer*. 2019;121(3):278–280. doi:10.1038/s41416-019-0515-5.
 8. Dai X, Gao Y, Wei W. Post-translational regulations of PD-L1 and PD-1: mechanisms and opportunities for combined immunotherapy. *Semin Cancer Biol*. 2022;85:246–252. doi:10.1016/j.semcancer.2021.04.002.
 9. Zhao P, Li L, Jiang X, Li Q. Mismatch repair deficiency/microsatellite instability-high as a predictor for anti-PD-1/PD-L1 immunotherapy efficacy. *J Hematol Oncol*. 2019;12(1):54. doi:10.1186/s13045-019-0738-1.
 10. McGrail DJ, Pilić PG, Rashid NU, Voorwerk L, Slagter M, Kok M, Jonasch E, Khasraw M, Heimberger AB, Lim B. et al. High tumor mutation burden fails to predict immune checkpoint blockade response across all cancer types. *Ann Oncol*. 2021;32(5):661–672. doi:10.1016/j.annonc.2021.02.006.
 11. Sehgal P, Chaturvedi P. Chromatin and cancer: implications of disrupted chromatin organization in tumorigenesis and its diversification. *Cancers Basel*. 2023;15(2):466. doi:10.3390/cancers15020466.
 12. Zhang FL, Li DQ. Targeting chromatin-remodeling factors in cancer cells: promising molecules in cancer therapy. *Int J Mol Sci*. 2022;23(21):12815. doi:10.3390/ijms232112815.
 13. Mohammad A, Jha S. Epimutations and their effect on chromatin organization: exciting avenues for cancer treatment. *Cancers Basel*. 2022;15(1):215. doi:10.3390/cancers15010215.
 14. Pan D, Kobayashi A, Jiang P, Ferrari de Andrade L, Tay RE, Luoma AM, Tsoucas D, Qiu X, Lim K, Rao P. et al. A major chromatin regulator determines resistance of tumor cells to T cell-mediated killing. *Sci*. 2018;359(6377):770–775. doi:10.1126/science.aao1710.
 15. Wang D, Wang J, Zhou D, Wu Z, Liu W, Chen Y, Chen G, Zhang J. SWI/SNF complex genomic alterations as a predictive biomarker for response to immune checkpoint inhibitors in multiple cancers. *Cancer Immunol Res*. 2023;11(5):646–656. doi:10.1158/2326-6066.CIR-22-0813.
 16. Zheng L, Liang X, Li S, Li T, Shang W, Ma L, Jia X, Shao W, Sun P, Chen C. et al. CHAF1A interacts with TCF4 to promote gastric carcinogenesis via upregulation of c-MYC and CCND1 expression. *EBioMedicine*. 2018;38:69–78. doi:10.1016/j.ebiom.2018.11.009.
 17. Wang D, Wang N, Li X, Chen X, Shen B, Zhu D, Zhu L, Xu Y, Yu Y, Shu Y. et al. Tumor mutation burden as a biomarker in resected gastric cancer via its association with immune infiltration and hypoxia. *Gastric Cancer*. 2021;24(4):823–834. doi:10.1007/s10120-021-01175-8.
 18. Duan R, Li X, Zeng D, Chen X, Shen B, Zhu D, Zhu L, Yu Y, Wang D. Tumor microenvironment status predicts the efficacy of postoperative chemotherapy or radiochemotherapy in resected gastric cancer. *Front Immunol*. 2021;11:609337. doi:10.3389/fimmu.2020.609337.
 19. Wang D, Chen X, Du Y, Li X, Ying L, Lu Y, Shen B, Gao X, Yi X, Xia X. et al. Associations of HER2 mutation with immune-related features and immunotherapy outcomes in solid tumors. *Front Immunol*. 2022;13:799988. doi:10.3389/fimmu.2022.799988.
 20. Lu Y, Li D, Cao Y, Ying L, Tao Q, Xiong F, Hu Z, Yang Y, Qiao X, Peng C. et al. A genomic signature reflecting fibroblast infiltration into gastric cancer is associated with prognosis and treatment outcomes of immune checkpoint inhibitors. *Front Cell Dev Biol*. 2022;10:862294. doi:10.3389/fcell.2022.862294.
 21. Kim ST, Cristescu R, Bass AJ, Kim KM, Odegaard JI, Kim K, Liu XQ, Sher X, Jung H, Lee M. et al. Comprehensive molecular characterization of clinical responses to PD-1 inhibition in metastatic gastric cancer. *Nat Med*. 2018;24(9):1449–1458. doi:10.1038/s41591-018-0101-z.
 22. Mariathasan S, Turley SJ, Nickles D, Castiglioni A, Yuen K, Wang Y, Kadel III EE, Koeppen H, Astarita JL, Cubas R. et al. TGF β attenuates tumour response to PD-L1 blockade by contributing to exclusion of T cells. *Nature*. 2018;554(7693):544–548. doi:10.1038/nature25501.
 23. Thorsson V, Gibbs DL, Brown SD, Wolf D, Bortone DS, Ou Yang TH, Porta-Pardo E, Gao GF, Plaisier CL, Eddy JA. et al. The immune landscape of cancer. *Immunity*. 2018;48(4):812–830. e14. doi:10.1016/j.immuni.2018.03.023.
 24. Wang D, Li X, Shen B, Chen X, Shu Y. Histone chaperone CHAF1A impacts the outcome of fluoropyrimidines-based adjuvant therapy in gastric cancer by regulating the expression of thymidylate synthetase. *Gene*. 2019;716:144034. doi:10.1016/j.gene.2019.144034.
 25. Li JC, Yang XR, Sun HX, Xu Y, Zhou J, Qiu SJ, Ke A, Cui Y, Wang Z, Wang W. et al. Up-regulation of Krüppel-like factor 8 promotes tumor invasion and indicates poor prognosis for hepatocellular carcinoma. *Gastroenterology*. 2010;139(6):2146–2157. e12. doi:10.1053/j.gastro.2010.08.004.
 26. Wang Y, Huang W, Wang N, Ouyang D, Xiao L, Zhang S, Ou X, He T, Yu R, Song L. et al. Development of arteannuin B sustained-release microspheres for anti-tumor therapy by integrated experimental and molecular modeling approaches. *Pharmaceutics*. 2021;13(8):1236. doi:10.3390/pharmaceutics13081236.
 27. Aran D, Hu Z, Butte AJ. xCell: digitally portraying the tissue cellular heterogeneity landscape. *Genome Biol*. 2017;18(1):220. doi:10.1186/s13059-017-1349-1.
 28. Yoshihara K, Shahmoradgoli M, Martínez E, Vegesna R, Kim H, Torres-García W, Treviño V, Shen H, Laird PW, Levine DA. et al. Inferring tumour purity and stromal and immune cell admixture from expression data. *Nat Commun*. 2013;4(1):2612. doi:10.1038/ncomms3612.
 29. Wu Z, Cui F, Yu F, Peng X, Jiang T, Chen D, Lu S, Tang H, Peng Z. Up-regulation of CHAF1A, a poor prognostic factor, facilitates cell proliferation of colon cancer. *Biochem Biophys Res Commun*. 2014;449(2):208–215. doi:10.1016/j.bbrc.2014.05.006.
 30. Tao L, Moreno-Smith M, Ibarra-García-Padilla R, Milazzo G, Drolet NA, Hernandez BE, Oh YS, Patel I, Kim JJ, Zorman B. et al. CHAF1A blocks neuronal differentiation and promotes neuroblastoma oncogenesis via metabolic reprogramming. *Adv Sci (Weinh)*. 2021;8(19):e2005047. doi:10.1002/adv.202005047.
 31. Tauriello D, Palomo-Ponce S, Stork D, Berenguer-Llargo A, Badiarmentol J, Iglesias M, Sevillano M, Ibiza S, Cañellas A, Hernandez-Momblona X. et al. TGF β drives immune evasion in genetically reconstituted colon cancer metastasis. *Nature*. 2018;554(7693):538–543. doi:10.1038/nature25492.
 32. Lin Y, Jing X, Chen Z, Pan X, Xu D, Yu X, Zhong F, Zhao L, Yang C, Wang B. et al. Histone deacetylase-mediated tumor microenvironment characteristics and synergistic immunotherapy in

- gastric cancer. *Theranostics*. 2023;13(13):4574–4600. doi:10.7150/thno.86928.
33. Shen C, Li M, Duan Y, Jiang X, Hou X, Xue F, Zhang Y, Luo Y. HDAC inhibitors enhance the anti-tumor effect of immunotherapies in hepatocellular carcinoma. *Front Immunol*. 2023;14:1170207. doi:10.3389/fimmu.2023.1170207.
 34. Hoek M, Stillman B. Chromatin assembly factor 1 is essential and couples chromatin assembly to DNA replication in vivo. *Proc Natl Acad Sci U S A*. 2003;100(21):12183–12188. doi:10.1073/pnas.1635158100.
 35. Sauer PV, Gu Y, Liu WH, Mattioli F, Panne D, Luger K, Churchill ME. Mechanistic insights into histone deposition and nucleosome assembly by the chromatin assembly factor-1. *Nucleic Acids Res*. 2018;46(19):9907–9917. doi:10.1093/nar/gky823.
 36. Sykaras AG, Pergaris A, Theocharis S. Challenging, accurate and feasible: CAF-1 as a tumour proliferation marker of diagnostic and prognostic value. *Cancers Basel*. 2021;13(11):2575. doi:10.3390/cancers13112575.
 37. Ayoub J, Buonanno M, Di Fiore A, De Simone G, Monti SM. Biochemical and structural insights into the Winged Helix Domain of P150, the largest subunit of the Chromatin Assembly Factor 1. *Int J Mol Sci*. 2022;23(4):2160. doi:10.3390/ijms23042160.
 38. Sun X, Ma Q, Cheng Y, Huang H, Qin J, Zhang M, Qu S. Overexpression of CHAF1A is associated with poor prognosis, tumor immunosuppressive microenvironment and treatment resistance. *Front Genet*. 2023;14:1108004. doi:10.3389/fgene.2023.1108004.
 39. Sun R, Xie HY, Qian JX, Huang YN, Yang F, Zhang FL, Shao Z-M, Li D-Q. FBXO22 possesses both protumorigenic and antimetastatic roles in breast cancer progression. *Cancer Res*. 2018;78(18):5274–5286. doi:10.1158/0008-5472.CAN-17-3647.
 40. Paltoglou S, Das R, Townley SL, Hickey TE, Tarulli GA, Coutinho I, Fernandes R, Hanson AR, Denis I, Carroll JS. et al. Novel Androgen Receptor Coregulator GRHL2 Exerts Both Oncogenic and Antimetastatic Functions in Prostate Cancer. *Cancer Res*. 2017;77(13):3417–3430. doi:10.1158/0008-5472.CAN-16-1616.
 41. Yuan F, Sun Q, Zhang S, Ye L, Xu Y, Deng G, Xu Z, Zhang S, Liu B, Chen Q. et al. The dual role of p62 in ferroptosis of glioblastoma according to p53 status. *Cell & Bioscience*. 2022;12(1):20. doi:10.1186/s13578-022-00764-z.
 42. Rozenberg JM, Zvereva S, Dalina A, Blatov I, Zubarev I, Luppov D, Bessmertnyi A, Romanishin A, Alsoulaiman L, Kumeiko V. et al. Dual role of p73 in cancer microenvironment and DNA damage response. *Cells*. 2021;10(12):3516. doi:10.3390/cells10123516.
 43. Jiang M, Jia K, Wang L, Li W, Chen B, Liu Y, Wang H, Zhao S, He Y, Zhou C. et al. Alterations of DNA damage response pathway: biomarker and therapeutic strategy for cancer immunotherapy. *Acta Pharm Sin B*. 2021;11(10):2983–2994. doi:10.1016/j.apsb.2021.01.003.
 44. Saxena S, Zou L. Hallmarks of DNA replication stress. *Mol Cell*. 2022;82(12):2298–2314. doi:10.1016/j.molcel.2022.05.004.
 45. Jiang P, Gu S, Pan D, Fu J, Sahu A, Hu X, Li Z, Traugh N, Bu X, Li B. et al. Signatures of T cell dysfunction and exclusion predict cancer immunotherapy response. *Nat Med*. 2018;24(10):1550–1558. doi:10.1038/s41591-018-0136-1.
 46. Zeng X, Zhou J, Xiong Z, Sun H, Yang W, Mok MTS, Wang J, Li J, Liu M, Tang W. et al. Cell cycle-related kinase reprograms the liver immune microenvironment to promote cancer metastasis. *Cell Mol Immunol*. 2021;18(4):1005–1015. doi:10.1038/s41423-020-00534-2.